

CASE PRESENTATION

Multimodality imaging can shift the clinical approach and prognosis of a patient: from heart failure and angina to cardiac amyloidosis

Alexandra Maria Chitroceanu¹, Alina Ioana Nicula^{2,3}, Roxana Cristina Rimbas^{1,2}, Mihaela Andreescu^{2,4}, Cristina Popp^{2,5}, Claudiu Stoicescu^{1,2}, Dragos Vinereanu^{1,2}

Abstract: AL (light chain) amyloidosis is a life threatening disease. Untreated patients with involvement of the heart, a condition known as cardiac amyloidosis (CA), tend to have the most rapid disease progression and worst prognosis. Therefore, it is essential to early recognize the signs of symptoms of CA, and to identify the affected individuals with readily available non-invasive tests, as timely therapy can prolong life. Different imaging tests are used to diagnose and stratify the risk of the disease noninvasively, and to follow-up of the disease course and response to therapy. In this light, we present a case of a woman with cardiovascular risk factors, initially admitted for typical angina and decompensated heart failure (HF), who was later diagnosed with AL amyloidosis with cardiac involvement, by using multimodality imaging assessment in a step-by-step fashion. This changed completely the prognosis of the patient. Timely chemotherapy and stem cell transplantation led to an improvement in clinical status, biomarkers, and in a regression of amyloid myocardial infiltration showed by imaging.

Keywords: multimodality, imaging, heart failure, angina, cardiac amyloidosis.

INTRODUCTION

AL (light chain) amyloidosis is a serious heterogeneous disease with a wide spectrum of non-specific clinical manifestations and a poor prognosis if left untreated¹. The prognosis is mainly determined by the presence and extent of cardiac involvement, a condition called cardiac amyloidosis (CA), as well as the response to therapy². Over the last years there has been remarkable progress in the diagnosis of cardiac amyloidosis, with a large body of emerging evidence for the clinical utility of various imaging modalities in achieving the diagnosis. However, the diagnosis of cardiac amyloidosis (CA) is often challenging, it relies on clinical awareness of and suspicion for the disease, and requires integration of data from a number of imaging modalities with clinical and serum biomarkers. Once the diagnosis of CA is established, a comprehensive approach (serial imaging with echocardiography and cardiac magnetic

resonance), in addition to clinical status and serum biomarkers, including NTproBNP and troponin, is recommended for risk stratification, prognosis and for monitoring cardiac disease progression and response to therapy¹. Timely chemotherapy and stem cell transplantation can lead to a significant clinical improvement, and regression of amyloid myocardial infiltration with a better prognosis³.

CASE PRESENTATION

A 57-year-old woman, experiencing typical angina at moderate exertion for one year, was admitted to our hospital. During the preceding month, she gradually developed resting dyspnoea and peripheral oedema. Patient's medical history was consistent with arterial hypertension, dyslipidaemia, and diabetes mellitus type 2 on diet. Current treatment included aspirin, perindopril 2.5 mg o.d., succinate metoprolol 50 mg o. d,

¹ Department of Cardiology and Cardiovascular Surgery, Emergency University Hospital, Bucharest, Romania

² „Carol Davila” University of Medicine and Pharmacy, Bucharest, Romania

³ Department of Radiology, Emergency University Hospital, Bucharest, Romania

⁴ Department of Hematology, Colentina Clinical Hospital, Bucharest, Romania

⁵ Department of Pathology, Colentina Clinical Hospital, Bucharest, Romania

► Contact address:

Roxana Cristina Rimbas, Department of Cardiology, Emergency University Hospital, „Carol Davila” University of Medicine 169 Splaiul Independentei, 050098, Bucharest, Romania.

E-mail: roxana.rimbas@umfcd.ro

and atorvastatin 20 mg o.d. Six months before admission, a transthoracic echocardiography detected left ventricular (LV) hypertrophy (interventricular septum, IVS=16 mm, and posterior wall thickness, PWT=15 mm), interpreted in the context of arterial hypertension, and preserved ejection fraction (LVEF = 50%).

On admission, physical exam found good general status, blood pressure of 130/90 mmHg without postural hypotension, regular heart rate of 75 bpm, with normal heart sounds, clear lung fields and mild pitting oedema of bilateral lower limbs.

Electrocardiogram (ECG) showed sinus rhythm, right atrial (RA) enlargement, diffuse low amplitude QRS complexes, pathological q wave in DIII with flatten T waves in inferior leads, and poor R wave progression in VI-V4 (Figure 1).

Serial testing of cardiac biomarkers indicated an increased level of NT-proBNP (11.400 pg/mL), along with constant mild elevated high-sensitive troponin I levels (hsTnI = 50 ng/L), and normal levels of serum creatine kinase myocardial band (CK-MB). Renal function was normal, without proteinuria.

Transthoracic echocardiography (TTE) revealed nondilated LV with severe concentric hypertrophy (IVS) =17 mm, PWT =16 mm, relative wall thickness (RWT) =0.8, LV mass =157 g/m², diffuse hypokinesia, a „ground-glass” appearance in the myocardium, and LV ejection fraction (LVEF) of 42%. A small pericardial effusion was present (Figure 2 A). Diastolic dysfunction (DD) was confirmed as grade III (E/A=3,

E= 97 cm/sec, E/E'= 25) with severely biatrial dilation (LA volume = 63 ml/m²; RA volume = 54 ml/m²) and mild to moderate mitral regurgitation (Figure 2 B, C and D). The right ventricle (RV) had an increase in wall thickness (free wall = 8 mm) and severely altered systolic function (TAPSE =8 mm, S'= 5 cm/sec) (Figure 3 A and B). Severe tricuspid regurgitation with pulmonary hypertension (estimated sPAP = 46 mmHg) was also noted (Figure 4 B). 2D speckle tracking echocardiography (STE) was used to quantify myocardial deformation. Global LV longitudinal peak systolic strain (GLS) was significantly impaired (-8.4%), with a severe altered deformation in all three layers, mainly at the basal and midventricular segments and relatively preserved at the apical level, resulting in a typical apical sparing strain pattern (Figure 4A).

Based on cardiovascular risk factors, clinical presentation (angina and heart failure), ECG and 2D TTE, coronary angiography was performed to exclude atherosclerotic coronary artery disease (CAD), and confirmed normal epicardial coronary artery.

Up to this point, the diagnosis was HF with mid-range EF, functional NYHA class IV, due to restrictive cardiomyopathy. Serum cardiac biomarkers were persistently elevated. Moreover, the pseudo-infarct pattern in the anterior and inferior leads on ECG, the discrepancy between low-voltage QRS and increased LV wall thickness on TTE, together with DD grade 3, and apical sparing pattern on STE were suggestive for CA. The patient underwent cardiac magnetic resonance

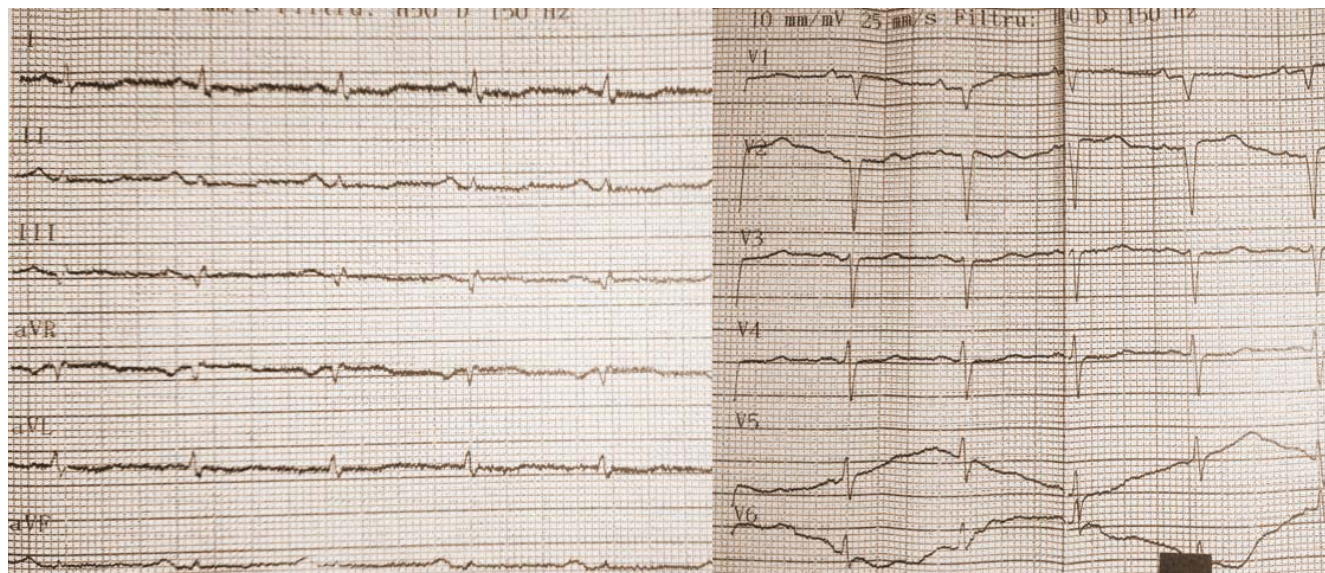


Figure 1. ECG image showing sinus rhythm, right atrial enlargement, low amplitude QRS complexes in limb leads, q wave in DIII with flatten T waves in inferior leads, and poor R wave progression in VI-V3.

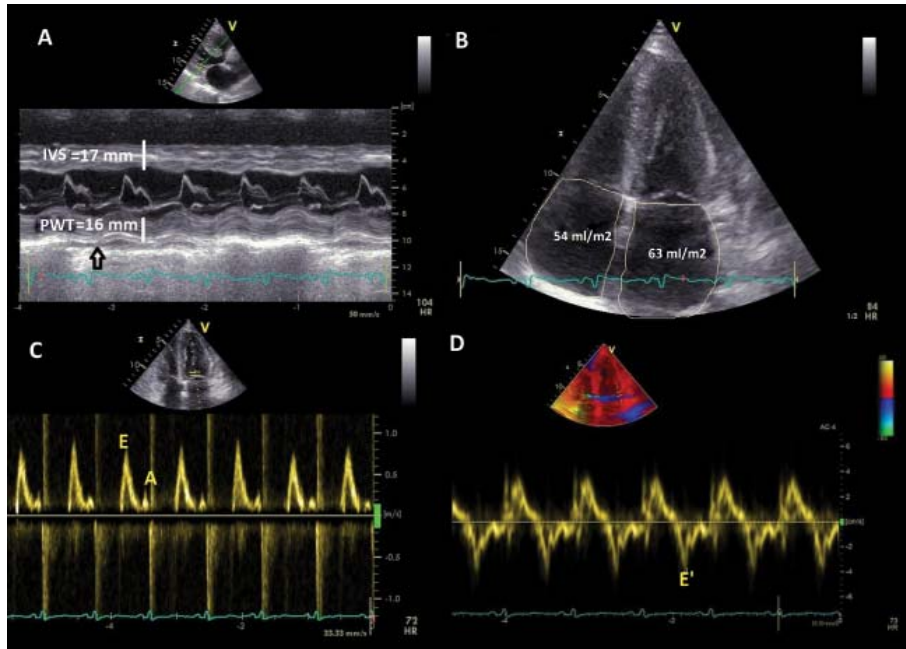


Figure 2. Transthoracic echocardiographic images for left ventricle showing A: severe concentric left ventricular hypertrophy (IVS=17 mm, PWT =16 mm, RWT =0.8, LV mass = 157 g/m²) B: biatrial dilatation (LA volume = 63 ml/m²; RA volume = 54 ml/m²) C and D: restrictive filling pattern (E/A=3, E=97 cm/sec, E' lateral = 4 cm/sec E'/E=25). IVS: interventricular septum; PWT: posterior wall thickness; RWT: relative wall thickness; LV: left ventricle; LA: left atrium; RA: right atrium. E=peak of early filling velocity; A=peak of late atrial filling velocity; E'lateral = lateral mitral annular peak early diastolic velocity.

(CMR) which confirmed LV hypertrophy and LVEF of 45%, non-dilated ventricles, enlarged atria (LAVi=66 ml/m²), and 5 mm pericardial effusion adjacent to LV lateral wall. CMR showed diffuse subendocardial late

gadolinium enhancement (LGE) at the base and mid-ventricle in the LV and along mitral and tricuspid valve, without LGE involvement of the LV apex and LA (Figure 5). An increase in RV wall thickness was also no-

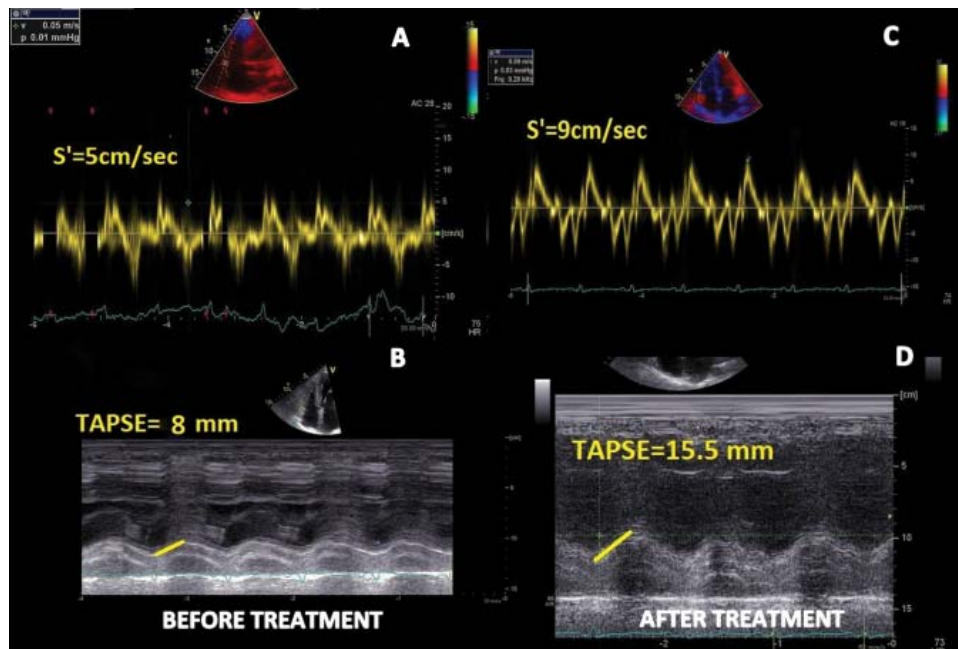


Figure 3. Transthoracic echocardiographic images for right ventricle before and after chemotherapy and stem cell transplantation. A and B (before treatment): altered longitudinal systolic function (TAPSE = 8 mm, S' = 5 cm/sec) at initial diagnosis; C and D (after treatment): improvement in longitudinal systolic (TAPSE = 15.5 mm, S' = 9 cm/sec) at 6 months follow up. TAPSE: tricuspid annular plane systolic excursion; s' = peak systolic velocity.

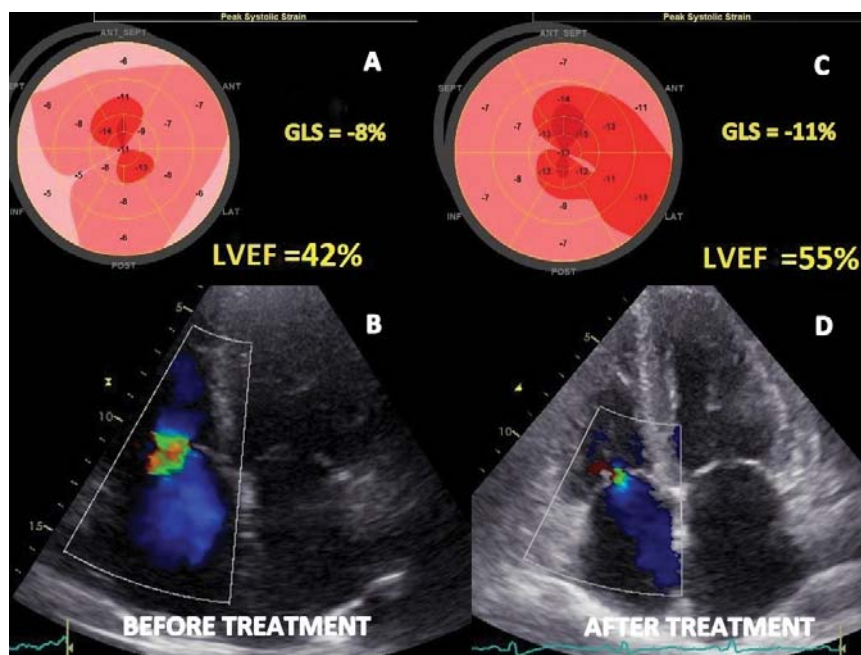


Figure 4. Transthoracic echocardiographic images before and after chemotherapy and stem cell transplantation. A and B (before treatment) images. **A:** Bull's eye plot image showing significantly reduced GLS (-8.4 %) with severe altered deformation mainly at the basal and midventricular segments and relatively preserved at the apex, with a typical apical sparing strain pattern or „cherry-on-top” pattern. **B:** severe tricuspid regurgitation on Colour Doppler images. C and D (after treatment) images. **C:** Bull's eye plot image showing an improvement in GLS (-11%) predominantly on the lateral and anterior wall. **D:** significantly regression of tricuspid regurgitation to mild by Colour Doppler images. GLS: global longitudinal strain.

ted but without LGE (Figure 6). The Query Amyloid Late Enhancement (QALE)12 score was 4 point, highly suggestive of cardiac AL amyloidosis. For histological confirmation, we decided to have a double biopsy, in order to increase sensitivity. Abdominal and rectal pad biopsy were taken and showed homogenous extracellular fibrils positive for Congo red staining and positive for green birefringence, specific for amyloid deposits (Figure 7). Once the diagnosis of CA was made, the next step was to identify the type of amyloid, in order to plan the appropriate treatment. Although serum and urine electrophoresis with immunofixation were negative, a serum free light chains assay showed a marked increase of λ light chains, indicating the presence of a population of plasma cells producing clonal λ free light chains. Because AL amyloidosis was suspected based on CMR findings, a bone marrow biopsy was performed and showed a medullary plasmacytosis (30%), a typical finding for AL amyloidosis.

For a complete work-up of the extension of the disease, an upper and lower limb electromyography was performed, which showed sensitive and motor peripheral neuropathy.

The final diagnosis was AL amyloidosis (primary amyloidosis) with cardiac involvement. Cardiac specific treatment included salt restriction, small doses of

diuretics (furosemide 20 mg o.d), and mineralocorticoid receptor antagonists (spironolactone 25 mg o.d) which led to a gradually improvement of congestion. We decided to continue treatment with metoprolol succinate 25 mg o.d, perindopril 2.5 mg o.d, and atorvastatin 20 mg o.d, well tolerated. Moreover, at this stage we agreed for no anticoagulation before haematological treatment. The patient was referred to a haematological centre and specific treatment with VCD (bortezomib-cyclophosphamide-dexamethasone) was started, as well as auto-stem-cell transplantation. All treatments were well tolerated, and no major side effects were observed. At 6 months follow up, the patient reported a significant improvement in her functional capacity, exercise tolerance, and presented a significantly decrease in NTproBNP level, up to 1500 pg/mL. A follow up TTE showed improvement of the LVEF from 42% to 55%, and of the GLS from -8% to -11% (Figure 4 A and C), decrease in the left and right atrial volumes (at follow up: LA = 40 ml/m² and RA = 30 ml/m²), and a significant regression of tricuspid regurgitation, from severe to moderate (Figure 4 B and D). Moreover, there was a significant improvement in the RV systolic function (TAPSE = 15.5 mm, S' = 9 cm/sec) (Figure 3 C and D), with a reduction in pulmonary hypertension (sPAP = 34 mmHg). All of these findings

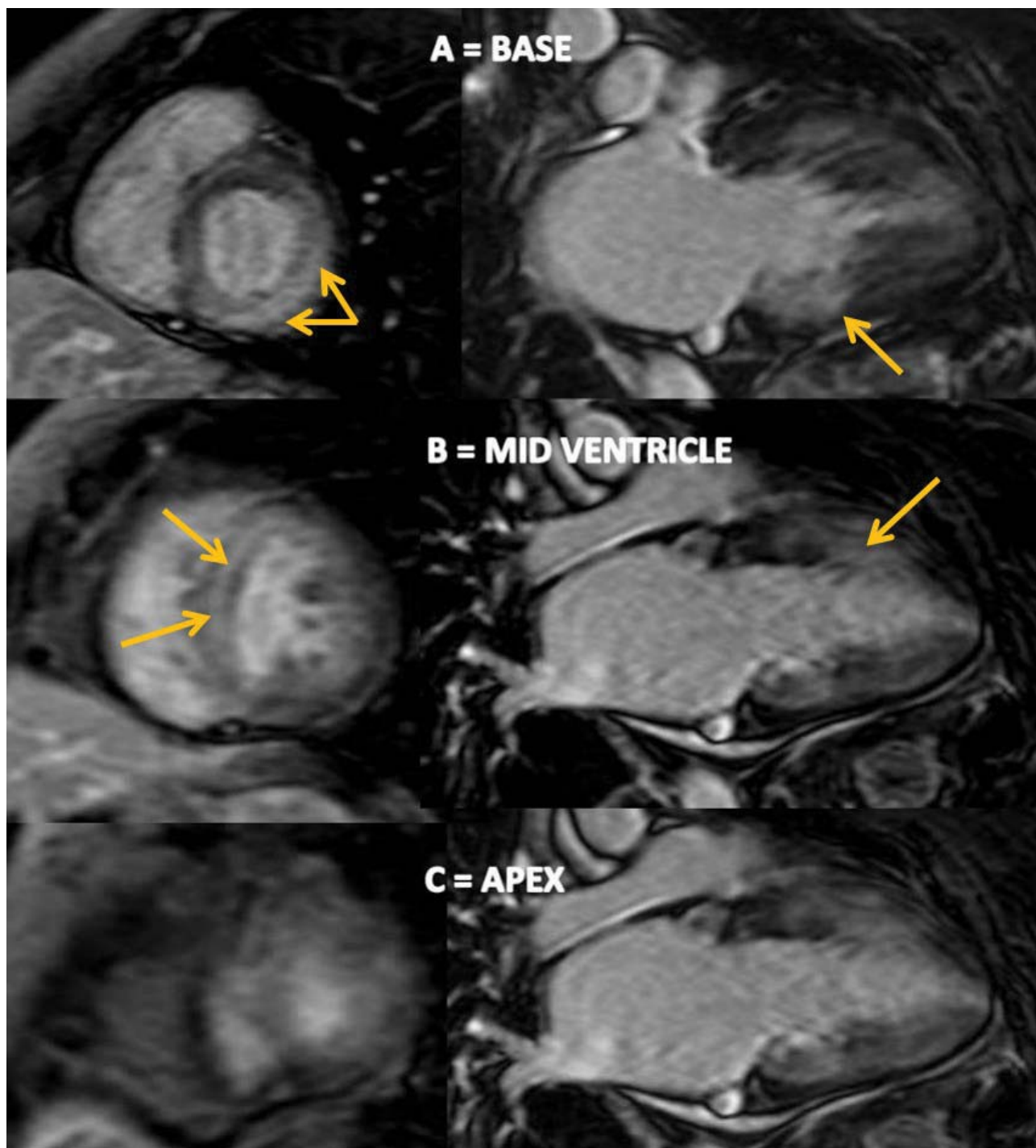


Figure 5. Cardiac magnetic resonance images showing A and B diffuse subendocardial LGE at the base and mid-ventricle in the left ventricle (yellow arrows). C no LGE of the apex. LGE: late-gadolinium enhancement.

suggested a regression of myocardial inflammatory λ light chains infiltrates as a result of chemotherapy response.

DISCUSSIONS

AL amyloidosis, the most common form of amyloidosis, occurs in the context of plasma cell dyscrasias

and other B-cell disorders, due to misfolded clonal immunoglobulin light chains¹. It is closely related to multiple myeloma, may overlap with it, and is treated with similar drugs¹. Theoretically, any organ can be infiltrated by light chains, except for the central nervous system. Approximately 50% of patients with AL amyloidosis have evidence of cardiac involvement at the

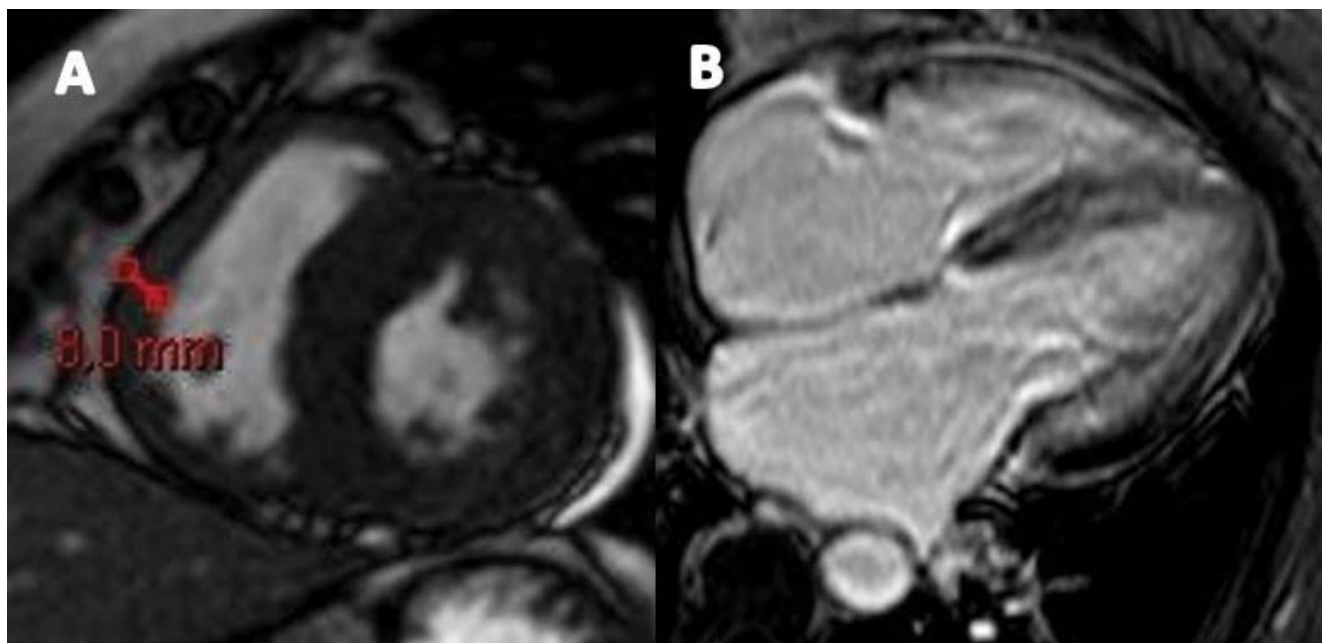


Figure 6. Cardiac magnetic resonance images showing A. an increase in right ventricle wall thickness (8 mm). B no LGE of the right ventricle. LGE: late-gadolinium enhancement.

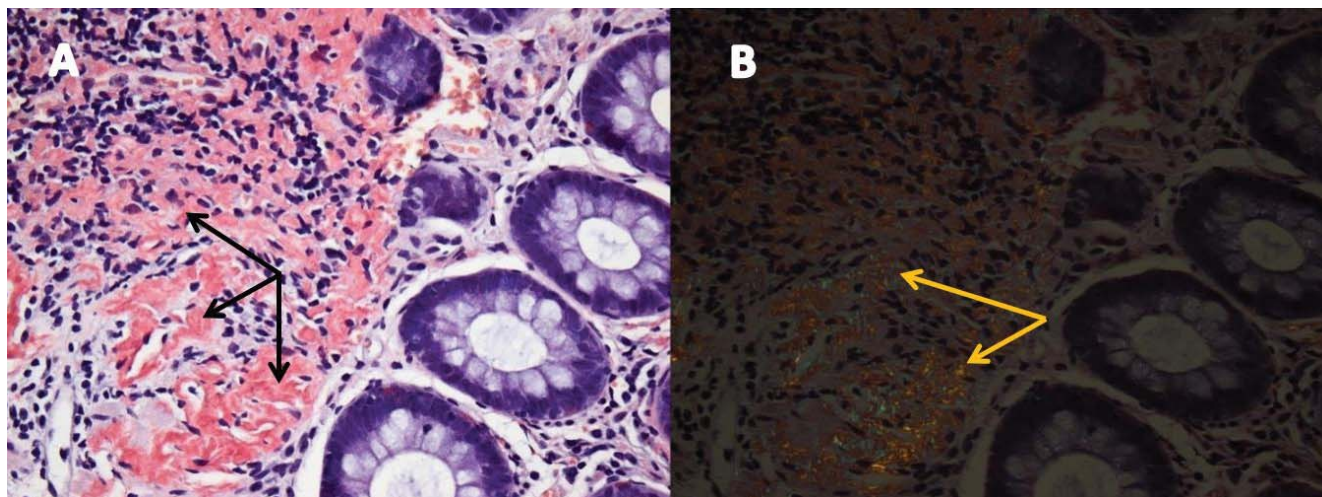


Figure 7. Rectal pad biopsy images showing A. homogenous extracellular fibrils positive for Congo red staining localized in the vascular walls (black arrows); B. These fibrils are positive for green birefringence, specific for amyloid deposits (yellow arrows).

initial evaluation, which is clinical significant in about 75%.^{2,3} Serum cardiac biomarkers troponin and BNP/NTproBNP are often persistently elevated in patients with CA, disproportionate to the degree of HF signs¹. Moreover, these biomarkers are frequently used for patients with cardiac AL amyloidosis for risk stratification, to better discriminate between groups with different outcomes, enabling better prognostic classification⁴. Survival decreases in patients with higher levels of troponin and NTproBNP. Patients with advanced

CA (elevated both troponin and NTproBNP levels) are often not considered for stem cell transplantation, because of high risk for transplantation-related mortality and poor overall survival⁴. Our patient had specific treatment with VCD and auto-stem-cell transplantation, with a positive outcome at 6-month follow up, and significant decrease of cardiac biomarkers and severity signs by TTE.

CA usually presents as a progressive biventricular HF, with right-sided signs frequently predominating².

Typical angina may occur on rare occasions, and might be due to exertion, leading to a misdiagnosis as CAD⁵. Moreover, pseudo-infarct pattern on ECG, a common finding in CA⁶, may mimic ischemic ECG changes, and clear differentiation can be challenging, as in our patient. This is particularly relevant in clinical practice, since a patient with additional cardiovascular risk factors who presents with angina and has a pseudo-infarct pattern on ECG may further demand coronary angiography in order to exclude atherosclerotic CAD. Previous studies have shown that patients with CA may experience anginal symptoms but have no significant atherosclerotic epicardial coronary disease.⁶ The explanation includes three possible mechanisms: vascular, extravascular and functional. Amyloid seems to accumulate in the walls of small coronary vessels, whereas the epicardial coronary arteries are normal with no amyloid deposition⁶. Secondly, perivascular and interstitial amyloid deposits might lead to extramural compression and reduced coronary perfusion time⁵. In addition, there might be a functional mechanism, due to coronary microvascular dysfunction with lower myocardial blood flow and lower coronary flow reserve⁷ even in the absence of epicardial coronary artery disease (CAD).

The diagnosis of AL amyloidosis is frequently challenging, particularly in the absence of systemic disease⁸, especially when a patient presents only with non-specific cardiac signs and symptoms, such as dyspnoea, fatigue and oedema. The key to diagnosis is a high index of suspicion and the final diagnosis of CA may require the integration of data from a number of imaging modalities², as in our patient. Echocardiography is usually the first imaging modality that might raise the suspicion of CA, but without any specific echocardiographic findings⁸. It is useful in the detection of gross morphological changes, such as the echogenic appearance of the myocardium, increased LV wall thickness (wall thickness ≥ 14 mm) in the absence of significant LV dilatation, and the presence of systolic and/or diastolic dysfunction⁹. In a patient with symptoms of congestive HF, findings of severe LV thickening should trigger the suspicion of CA, especially if there is a discordance between wall thickness on echocardiogram and QRS voltage on ECG³. Diastolic dysfunction is attributed to increased stiffness in the myocardium, as a result of amyloid deposition, which progresses with the degree of myocardial infiltration, ranging from impaired relaxation to a restrictive pattern in patients with advanced disease⁸, like in our case. A restrictive

diastolic pattern should prompt a broader differential diagnosis with other restrictive cardiomyopathies³. CA should be suspected in any patient with symptoms or signs of unexplained HF, especially when LV wall thickness is significantly increased and a prominent diastolic dysfunction is present⁹. All these findings were present and raised suspicion of amyloidosis in our patient. Moreover, STE revealed an 'apical sparing' or a 'cherry-on-top' pattern on the bull's eye plot of GLS. This is a sensitive and specific finding that can be used to distinguish amyloidosis from other causes of LV hypertrophy¹⁰ n=15 with aortic stenosis.

Multiple echocardiographic parameters have shown prognostic value in patients with CA¹¹ myocardial contraction fraction, and tricuspid annular plane systolic excursion (TAPSE). Conventional measurements such as increased wall thickness², decreased LVEF₄, restrictive diastolic pattern (increased E/E' ratio, LA dilatation)¹² and right ventricle failure¹³ were attributed to a reduced overall survival when studied in isolation. Recently, there is an increased level of evidence that GLS₄ and right ventricle dysfunction¹¹ myocardial contraction fraction, and tricuspid annular plane systolic excursion (TAPSE) are independent prognostic markers in patients with AL CA. The degree of LV and RV dysfunction appears to gradually decrease with the degree of myocardial infiltration. RV dysfunction may occur in amyloidosis as a consequence of LV impairment or due to direct RV subendocardial amyloid infiltration⁴. Thus, the prognostic role of the RV dysfunction is linked to whether there is a RV amyloid infiltration. Moreover, it has been validated that GLS may provide additional information survival among patients treated with stem cell transplantation, beyond the well-validated cardiac biomarkers (NT-proBNP and troponin) A cut off of -17% was identified as the value that best discriminated survivors from no survivors⁴. Taking into consideration the GLS value and the NTproBNP seric level, we consider that our patients carries a poor prognosis.

CMR is also useful for diagnosing CA, particularly when performed with the use of the gadolinium as an imaging agent⁹. In amyloidosis, LGE can occur in 3 possible patterns: no LGE, sub-endocardial enhancement, and transmural enhancement¹⁴. The pattern of LGE may help in differentiating the two subtypes of CA, with transmural LGE being more prevalent in TTR amyloidosis as opposed to sub-endocardial LGE, which appears to be more prevalent in AL amyloidosis¹⁴. Moreover, the Query Amyloid Late Enhancement

(QALE) score was recently validated as a prognostic score in patients with AL amyloidosis¹⁴. QALE score was based on patterns of LGE in the LV at 3 levels (base, mid ventricle, and apex) and in the RV free wall. The maximum LV LGE score at each level is 4 (maximum LV LGE score 12), plus 6 if RV LGE is present and ranged from 0 (no LGE in the left or right ventricle) to 18 (global transmural LV LGE with RV involvement)¹⁴. A cut-off of 9 was proved to differentiate prognosis in AL amyloidosis patients with a subendocardial LGE pattern¹⁵. Patients with a subendocardial LGE-QALE score < 9 have a better prognosis, similar to the patients with no apparent cardiac involvement and no LGE, whereas a value ≥ 9 implies a worse prognosis, similar to the transmural LGE¹⁵. CMR showed subendocardial LGE in our patient, highly suggestive for AL amyloidosis, and the QALE score was 4, with subendocardial LGE observed at the base and mid-cavity of LV, without RV LGE.

Based on TTE and STE, a restrictive cardiomyopathy due to an infiltrative disease was suspected, with a high index of suspicion for CA. CMR pointed toward AL amyloidosis based on subendocardial LGE distribution, which was further confirmed by abdominal fat, rectal and bone marrow biopsy, as well as serum free light chains assay.

If left untreated, the median survival in AL cardiac amyloidosis with elevated levels of serum cardiac biomarkers (troponin and NT-proBNP) is between 14 and 5.8 months¹. Therefore, timely diagnosis and initiation of therapy are essential to improve patient's outcome. Cardiac response to therapy is defined by changes in cardiac biomarkers, NYHA class, and imaging parameters¹. Initially, increased levels of serum cardiac biomarkers (troponin and NT-proBNP), together with echocardiographic markers (severe concentric hypertrophy, grade III diastolic dysfunction, decreased RV longitudinal function and reduced GLS) indicated a poor prognosis. However, subendocardial LGE located at the basal and mid LV, the absence of RV involvement, and a QALE score of 4 attributed a better overall survival. This was certified at 6 month follow up, after chemotherapy and stem cell transplantation, by evident improvement in clinical status, biomarkers, and right and left systolic function by echocardiography. The improvement in cardiac biomarkers and function could be secondary to a regression in myocardial inflammatory λ light chains infiltrates as a result of chemotherapy response, which attributed a better prognosis of this patient. This explanation is

consistent with recent studies that showed that intramyocardial inflammation by endomyocardial biopsy correlated with disease progression and increased mortality in patients with AL amyloidosis¹⁶.

CONCLUSION

Cardiac amyloidosis may have various clinical presentations, and diagnosis relies mainly on a high level of suspicion based on the clinical setting, cardiac biomarkers, and non-invasive imaging tests, especially transthoracic echocardiography and cardiac magnetic resonance. Our case highlights important clues that pointed toward the diagnosis of this disease. In order to confirm the diagnosis and to start the appropriate treatment, evidence of amyloid in tissues was required. Early diagnosis combined with timely chemotherapy and stem cell transplantation lead to disease stabilization and a significant improvement in patient status. Careful consideration of various imaging tests was needed to clarify suspicion, to diagnose the disease noninvasively, and follow-up the course of the disease.

Conflict of interest: none declared.

References:

1. Fine NM, Davis MK, Anderson K, et al. Canadian Cardiovascular Society/Canadian Heart Failure Society Joint Position Statement on the Evaluation and Management of Patients With Cardiac Amyloidosis. *Canadian Journal of Cardiology*. 2020;36(3):322-334.
2. Khanna S, Wen I, Bhat A, et al. The Role of Multi-modality Imaging in the Diagnosis of Cardiac Amyloidosis: A Focused Update *Frontiers in Cardiovascular Medicine*. 2020;7:212.
3. Kittleson MM, Maurer MS, Ambardekar AV, et al. Cardiac Amyloidosis: Evolving Diagnosis and Management: A Scientific Statement From the American Heart Association. *Circulation*. 2020;142(1):7-22.
4. Pun SC, Landau HJ, Riedel ER, et al. Prognostic and Added Value of Two-Dimensional Global Longitudinal Strain for Prediction of Survival in Patients with Light Chain Amyloidosis Undergoing Autologous Hematopoietic Cell Transplantation. *Journal of the American Society of Echocardiography*. 2018;31(1):64-70.
5. Nguyen HT, Nguyen CTH. Cardiac amyloidosis mimicking acute coronary syndrome: a case report and literature review. *European Heart Journal - Case Reports*. October 2020.
6. Neben-Wittich MA, Wittich CM, Mueller PS, Larson DR, Gertz MA, Edwards WD. Obstructive intramural coronary amyloidosis and myocardial ischemia are common in primary amyloidosis. *The American Journal of Medicine*. 2005;118(11):1287.
7. Dorbala S, Vangala D, Bruyere J, et al. Coronary Microvascular Dysfunction Is Related to Abnormalities in Myocardial Structure and Function in Cardiac Amyloidosis. *JACC: Heart Failure*. 2014;2(4):358-367.
8. Agha AM, Parwani P, Guha A, et al. Role of cardiovascular imaging for the diagnosis and prognosis of cardiac amyloidosis. *Open heart*. 2018;5(2):e000881-e000881.
9. Quarta CC, Kruger JL, Falk RH. Cardiac Amyloidosis. *Circulation*. 2012;126(12):178-182.
10. Phelan D, Collier P, Thavendiranathan P, et al. Relative apical sparing of longitudinal strain using two-dimensional speckle-tracking echocardiography is both sensitive and specific for the diagnosis of cardiac amyloidosis. *Heart*. 2012;98(19):1442 - 1448.

Multimodality imaging can shift the clinical approach and prognosis of a patient

11. Knight DS, Zumbo G, Barcella W, et al. Cardiac Structural and Functional Consequences of Amyloid Deposition by Cardiac Magnetic Resonance and Echocardiography and Their Prognostic Roles. *JACC: Cardiovascular Imaging*. 2019;12(5):823-833.
12. Child N, Muhr T, Sammut E, et al. Prevalence of myocardial crypts in a large retrospective cohort study by cardiovascular magnetic resonance. *Journal of Cardiovascular Magnetic Resonance*. 2014;16(1):66.
13. Bodez D, Ternacle J, Guellich A, et al. Prognostic value of right ventricular systolic function in cardiac amyloidosis. *Amyloid*. 2016; 23(3):158-167.
14. Dungu JN, Valencia O, Pinney JH, et al. CMR-Based Differentiation of AL and ATTR Cardiac Amyloidosis. *JACC: Cardiovascular Imaging*. 2014;7(2):133-142.
15. Wan K, Sun J, Han Y, et al. Increased Prognostic Value of Query Amyloid Late Enhancement Score in Light-Chain Cardiac Amyloidosis. *Circulation Journal*. 2018;82(3):739-746.
16. Siegismund, C.S., Escher, F., Lassner, D, et al. Intramyocardial inflammation predicts adverse outcome in patients with cardiac AL amyloidosis. *Eur J Heart Fail*, 2018: 751-757.